

# Threshold enhancement in $\eta$ photoproduction from ${}^2\text{H}$ and ${}^4\text{He}$

V. Hejny<sup>1</sup>, J. Weiß<sup>2</sup>, P. Achenbach<sup>3</sup>, J. Ahrens<sup>3</sup>, J.R.M. Annand<sup>4</sup>, R. Beck<sup>3</sup>, M. Kotulla<sup>2</sup>, B. Krusche<sup>5,a</sup>, V. Kuhr<sup>6</sup>, R. Leukel<sup>3</sup>, I.J.D. MacGregor<sup>4</sup>, V. Metag<sup>2</sup>, R. Novotny<sup>2</sup>, V. Olmos de León<sup>3</sup>, F. Rambo<sup>6</sup>, A. Schmidt<sup>3</sup>, M. Schumacher<sup>6</sup>, U. Siodlaczek<sup>7</sup>, H. Ströher<sup>1</sup>, F. Wissmann<sup>6</sup>, and M. Wolf<sup>2</sup>

<sup>1</sup> Institut für Kernphysik, Forschungszentrum Jülich, D-52425, Jülich, Germany

<sup>2</sup> II. Physikalisches Institut, Universität Gießen, D-35392 Gießen, Germany

<sup>3</sup> Institut für Kernphysik, Universität Mainz, D-55099 Mainz, Germany

<sup>4</sup> Department of Physics and Astronomy, University of Glasgow, Glasgow G128QQ, UK

<sup>5</sup> Department of Physics and Astronomy, University of Basel, Ch-4056 Basel, Switzerland

<sup>6</sup> II. Physikalisches Institut, Universität Göttingen, D-37073 Göttingen, Germany

<sup>7</sup> Physikalisches Institut, Universität Tübingen, D-72076 Tübingen, Germany

Received: 23 November 2001 / Revised version: 27 January 2002  
Communicated by M. Garçon

**Abstract.** The photoproduction of  $\eta$ -mesons from  ${}^2\text{H}$  and  ${}^4\text{He}$  has been studied for energies close to the production thresholds. The experiments were carried out with the tagged photon beam of the Mainz MAMI accelerator. The  $\eta$ -mesons were detected via their two photon decays with the electromagnetic calorimeter TAPS. Total cross-sections, angular and momentum distributions of the  $\eta$ -mesons have been determined for both reactions. The total cross-sections in the threshold region show a large enhancement over the predictions of a participant-spectator model, indicating significant final-state interaction effects. The results are compared to recent model calculations taking into account nucleon-nucleon and nucleon- $\eta$  final-state interaction effects on different levels of sophistication.

**PACS.** 13.60.Le Meson production – 14.40.Aq  $\pi$ ,  $K$  and  $\eta$  mesons – 25.20.Lj Photoproduction reactions

## 1 Introduction

The interaction of mesons with nucleons and nuclei is one of the central issues in strong interaction physics. Detailed experimental and theoretical studies of the pion-nucleon and pion-nucleus interaction have largely contributed to this field. However, much less is known in the case of the heavier pseudoscalar mesons, the  $\eta$ - and  $\eta'$ -mesons, which due to their short lifetimes are not available as beams. In particular, the  $\eta$ -meson has recently attracted much interest. At small meson-nucleon relative momenta the situation for  $\eta$ -mesons and pions is very different. This is due to the fact that an  $s$ -wave nucleon resonance, the  $S_{11}(1535)$ , which is located very closely to the production threshold for  $\eta$ -mesons, couples strongly to the  $N\eta$  system. As a consequence, reactions like photoproduction of  $\eta$ -mesons are completely dominated by the excitation of this resonance [1]. This feature of the  $N\eta$  system has consequences for the interaction of  $\eta$ -mesons with nuclei. It has even been argued [2] that due to the  $N\pi$ - $N\eta$  interaction in the  $S_{11}$  state the  $NN\eta$  system might be bound.

Most information of the  $N\eta$  interaction, in particular the  $\eta$ -nucleon scattering length, has been extracted from

coupled-channel analyses of pion- and photon-induced meson production reactions. Already in 1985 Bhalerao and Liu [3] found an attractive  $s$ -wave  $N\eta$  interaction with a scattering length of  $a_\eta = (0.27 + 0.22i)$  fm from such an analysis. Shortly afterwards, Liu and Haider [4] pointed out that for nuclei with  $A > 10$  this interaction might lead to the formation of bound  $\eta$ -nucleus states which they termed  $\eta$ -mesic nuclei. Experimental evidence for such “heavy”  $\eta$ -mesic nuclei was sought in different reactions [5–7], but so far with non-conclusive results.

Substantial progress has been achieved during the last few years in the experimental study of  $\eta$  production reactions. Precise experiments using hadron-induced reactions (*e.g.*, at CELSIUS, COSY, SATURNE) [8–15] or photon-induced reactions (*e.g.*, at ELSA, GRAAL, JLAB, KEK, MAMI) [1, 16–23] on the free nucleon and on nuclei have vastly improved the available data base. The new results for the elementary reactions on the nucleon, in particular for the photon-induced reaction [1], have prompted several groups to reanalyse the  $\eta N$  interaction [24–29]. They found  $N\eta$  scattering lengths with real parts in the range 0.5–1. fm, considerably larger than the original result from Bhalerao and Liu [3]. Furthermore, strong threshold enhancements were observed in hadron-induced  $\eta$  produc-

<sup>a</sup> e-mail: Bernd.Krusche@unibas.ch

tion reactions. In the following, the possible existence of  $\eta$ -nucleus bound states for the light nuclei  ${}^2\text{H}$ ,  ${}^3\text{H}$ ,  ${}^3\text{He}$  and  ${}^4\text{He}$  was intensely discussed in the literature [12, 25, 30–35], but there is still some controversy regarding the necessary strength of the  $\eta N$  interaction.

The investigation of  $\eta$  production reactions from light nuclei in the threshold region is a very useful tool for the study of  $\eta$ -nucleus interactions. The idea is, that final-state interaction (FSI) of the  $\eta$ -meson with the nucleus, in particular the formation of quasibound states in the vicinity of the production threshold, will give rise to an enhancement of the cross-section relative to the expectation for phase space behavior. Such deviations can also arise from FSI effects between the nucleons, which are not related to the  $\eta N$  interaction, so that the interpretation of the results needs at least reliable model calculations which account for these trivial effects. During the past five years  $\eta$  production near threshold was intensively investigated in the reactions:  $pp \rightarrow pp\eta$  [10],  $np \rightarrow d\eta$  [9, 11],  $pd \rightarrow \eta{}^3\text{He}$  [8],  $dd \rightarrow \eta{}^4\text{He}$  [12], and  $pd \rightarrow pd\eta$  [13]. All reactions show more or less pronounced threshold enhancements.

Possible  $\eta$ -nucleus FSI effects should show up independently of the initial state of the reaction. Photoproduction of  $\eta$ -mesons from light nuclei is a clean tool for the preparation of the  $\eta$ -nucleus final state with small relative momenta, but due to the small electromagnetic cross-sections no sensitive threshold measurements have been reported until now. Previously,  $\eta$  photoproduction from the deuteron was studied in two experiments carried out at the MAMI and ELSA accelerators [16, 18], which aimed at the extraction of the isospin composition of the electromagnetic excitation of the  $S_{11}(1535)$  resonance. Both experiments did not reach the statistical accuracy necessary for a sensitive search for threshold effects. In the present paper, we report the results from a new measurement of the  $d(\gamma, \eta)X$  reaction with an improvement in counting statistics by one order of magnitude compared to ref. [16] and the first measurement of the threshold behavior of  $\eta$  photoproduction from  ${}^4\text{He}$ . The data have been measured as part of a systematic investigation of  $\eta$  photoproduction from light nuclei. The results from the  ${}^4\text{He}$  measurement concerning the isospin structure of the  $S_{11}(1535)$  excitation have been published in ref. [36].

The excitation of the  $S_{11}(1535)$  resonance, which dominates  $\eta$ -threshold production, involves an electromagnetic spin-flip transition which is predominantly of isovector nature. The isoscalar admixture in the amplitude contributes only at the 10% level [16, 18, 22, 36]. Consequently, coherent  $\eta$  photoproduction, where the nucleus remains in the ground state, is suppressed for the  $J = 1, I = 0$  deuteron [18, 22] and almost entirely forbidden for the  $I = J = 0$  nucleus  ${}^4\text{He}$  [36]. As a result inclusive reactions are dominated by incoherent breakup processes. Nevertheless, close to threshold, energy conservation requires that the kinematical conditions must be similar to the coherent process. The relative momentum of the  $np$  pair in the  $\gamma d \rightarrow \eta np$  reaction must be small so that nucleon-nucleon FSI will certainly be important.

## 2 Experiment and analysis

Eta photoproduction from the deuteron and  ${}^4\text{He}$  was measured close to the production thresholds at  $E_\gamma = 627$  MeV and 587 MeV, respectively. The experiments were carried out at the Glasgow tagged photon facility [37] installed at the Mainz Microtron (MAMI) [38] with the electromagnetic calorimeter TAPS [39, 40]. A detailed description of the setup and the analysis is given in [36]. Here, we summarize only the most relevant aspects of the data analysis. The identification of photons was done with a time-of-flight measurement with typically 500 ps resolution (FWHM), the pulse-shape discrimination capability of the  $\text{BaF}_2$  scintillators, and the plastic scintillators mounted as charged-particle veto detectors in front of the  $\text{BaF}_2$  crystals. The combination of these methods assures that contaminations from particles are below the 1% level. The  $\eta$ -mesons were then identified with a standard invariant-mass analysis of coincident photon pairs using

$$m_{\text{inv}}^2 = (E_1 + E_2)^2 - (\mathbf{p}_1 + \mathbf{p}_2)^2 = 2E_1 E_2 (1 - \cos \Phi_{12}), \quad (1)$$

where  $E_i$  denotes the energies,  $\mathbf{p}_i$  the momenta of the two photons and  $\Phi_{12}$  the relative angle between them. Background in the invariant-mass spectra originated only from events of multiple  $\pi^0$  photoproduction [36] when two photons from different pions were observed and the other photons escaped detection due to the limited solid angle coverage of the detector. However, as shown with Monte Carlo simulations [36], in the invariant-mass spectra this background levels off under the low-energy tail of the  $\eta$  peak and can thus be removed with a cut on the invariant mass. The fact that the excitation functions for  $\eta$  photoproduction (see fig. 2 in the following) are consistent with zero below the respective  $\eta$  production thresholds is a further evidence that this background was completely removed by the invariant-mass cut.

The detection efficiency of the TAPS-detector for  $2\gamma$ -decays of  $\eta$ -mesons was determined with Monte Carlo simulations based on the GEANT-code [41]. It was previously demonstrated [40] that this simulations reproduce the photon response of the detector very precisely. The detection efficiency  $\epsilon_\eta(\Theta_\eta, T_\eta)$  depends only on the laboratory polar angle  $\Theta_\eta$  and the laboratory kinetic energy  $T_\eta$  of the  $\eta$ -mesons, which were both measured in the experiment. The efficiency was not large due to the limited solid angle coverage. However, in the investigated range of incident photon energies it was not zero for any kinematically possible combination of  $\Theta_\eta$  and  $T_\eta$ , because always some fraction of the decay photon pairs was in the acceptance of the calorimeter. This is demonstrated in fig. 1, where for one range of incident photon energies the detector efficiency and the measured distribution of  $\eta$ -mesons are compared. Therefore, no model assumptions were needed for the determination of the efficiency correction. It was obtained from the Monte Carlo simulations as a function of  $\Theta_\eta$  and  $T_\eta$  and corrected event by event. Finite-resolution effects were accounted for in an iterative procedure: in a first step  $\epsilon_\eta$  was simulated with an isotropic angular and energy distribution of the  $\eta$ -mesons. This efficiency was

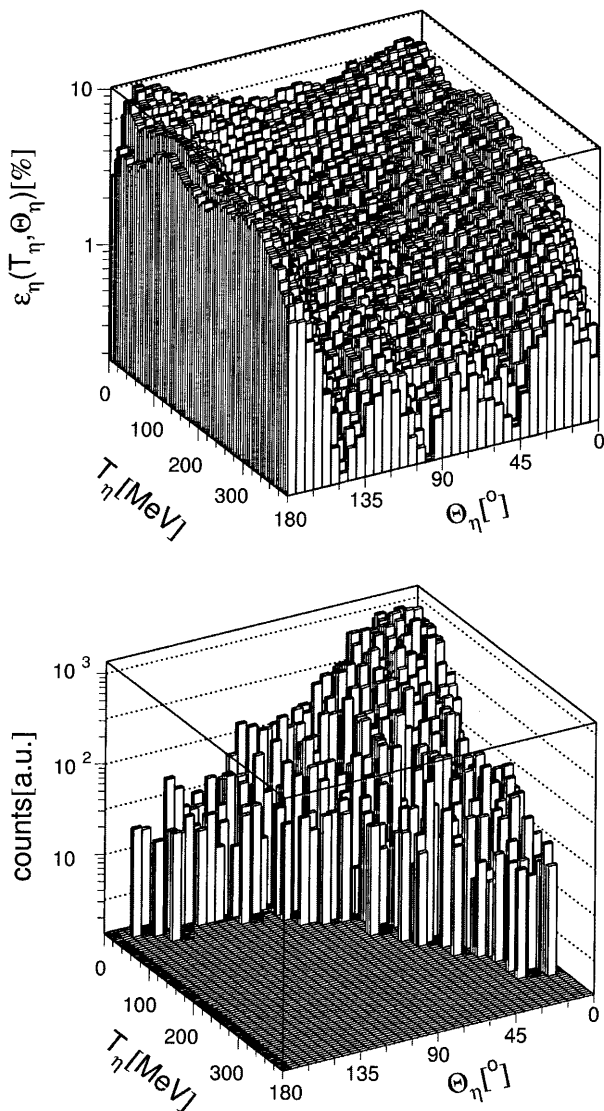


**Fig. 1.** Detector acceptance for  $\eta$ -mesons as a function of the laboratory polar angle and the laboratory kinetic energy of the mesons. Upper part: efficiency calculated with Monte Carlo simulation. Lower part: measured distribution of  $\eta$ -mesons for incident photon energies 660–680 MeV.

then used to correct the data and in the following the distributions extracted from the data were used as input for the simulations. This procedure converged after 1-2 iterations. The efficiency correction for the total cross-section determined this way varies smoothly between 6.5–5% for the first 50 MeV of incident photon energies above the production thresholds. The systematic uncertainty of the efficiency is below 5%. This uncertainty has been investigated in detail for the  $\gamma p \rightarrow p\eta$  reaction [42]. In this case the  $3\pi^0$ -decay of the  $\eta$ -meson was analysed in addition to the  $2\gamma$ -decay. The two decay channels have very different detection efficiencies both on an absolute scale as well as for the energy dependence. The energy dependence of the excitation functions extracted from the two decay channels agreed within the statistical uncertainties

of a few per cent. The absolute value of the cross-section ratio was consistent with previous measurements of the ratio of the decay widths  $\Gamma_{\eta \rightarrow 2\gamma} / \Gamma_{\eta \rightarrow 3\pi^0}$  but had even a smaller uncertainty.

The absolute normalization of the cross-sections was obtained from the target thicknesses and the intensity of the photon beam. The latter was determined by counting the deflected electrons in the tagging spectrometer and measuring the tagging efficiency (*i.e.*, the fraction of the correlated photons which pass through the photon collimator) by moving a BGO-detector into the photon beam at reduced intensity. The uncertainty of this normalization is estimated as 3%.

The threshold behavior of  $\eta$  photoproduction was studied in inclusive experiments where only the  $\eta$ -mesons were detected. Exclusive measurements of quasifree  $\eta$  photoproduction from the neutron via coincident detection of recoil nucleons at higher incident photon energies [36] and an exclusive measurement of coherent  $\eta$  photoproduction from the deuteron via coincident detection of the recoil deuterons [22] are reported elsewhere.

### 3 Results and discussion

The measured total cross-sections are shown in fig. 2. In the helium case, the data are consistent with zero at incident photon energies below the breakup threshold. This agrees with the expectation that the cross-section of the coherent reaction is negligible. A small coherent contribution might be visible for the deuteron between the coherent and breakup thresholds. For deuterium also the older data [16] with larger statistical errors is shown. The two data sets are in good agreement within their statistical uncertainties. Very close to threshold both data sets might exhibit a structure, which however is not statistically significant.

In a first step the data are compared with a simple participant-spectator model in the impulse approximation. This model assumes that the ratio  $\sigma_n / \sigma_p$  of the cross-sections for  $\eta$  photoproduction from the proton and the neutron is constant over the investigated energy range. A Breit-Wigner fit to the proton data [1,16] was folded with the momentum distribution of the bound nucleons and normalized to the nuclear data by a constant factor representing the cross-section ratio  $\sigma_n / \sigma_p$ . The momentum distributions of the nucleons were generated from the deuteron [43] and helium wave functions. The latter was calculated from the measured  $^4\text{He}$  charge form factor [44]. The proton form factor was unfolded and the proton spatial density was generated via a Fourier transformation. The spatial wave function was taken as square root of the density distribution and the wave function in momentum space was calculated from a second Fourier transformation. This is based on the assumptions that  $^4\text{He}$  is purely  $s$ -wave and protons and neutrons have the same distributions. As already reported in [16,36] good agreement between model and data over a large energy range is obtained in both cases under the assumption that

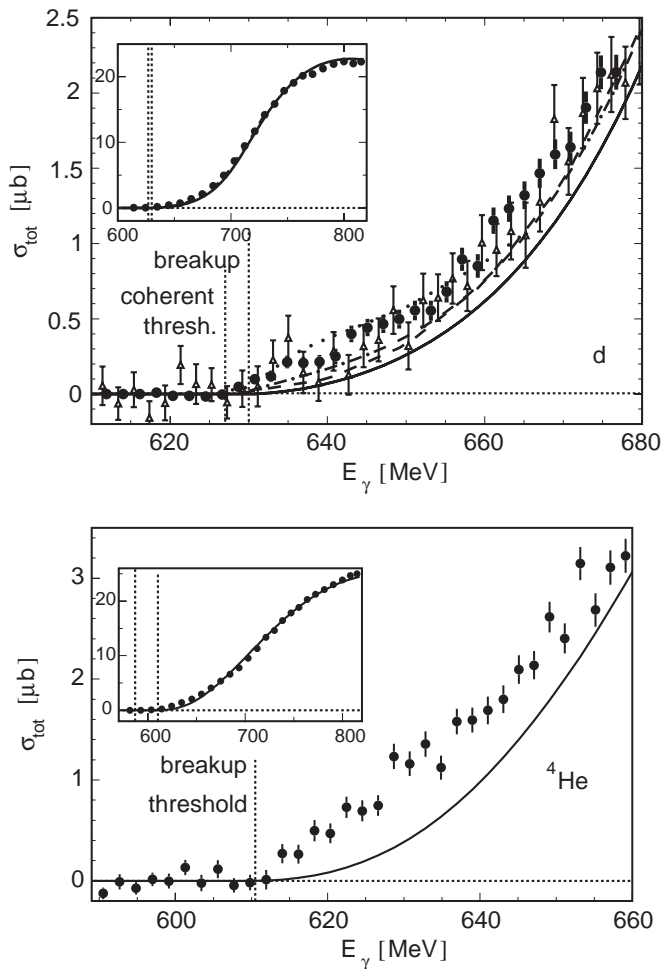


**Fig. 2.** Total cross-sections for  $\eta$  photoproduction from the deuteron (upper part) and  ${}^4\text{He}$  (bottom part). Main plots: threshold region; insets: full measured energy range. The dashed vertical lines indicate the coherent and quasifree thresholds. Solid curves: impulse approximation. For deuteron: open triangles: data from ref. [16] dash-dotted curve: model with  $NN$  FSI (Sibirtsev *et al.* [45]), dashed curve: model with first-order  $NN$  and  $\eta N$  FSI (Fix *et al.* [46]), dotted curve: three-body model (Fix *et al.* [47]).

$\sigma_n/\sigma_p \approx 0.66$ . This result also agrees with exclusive experiments where the cross-section ratio is determined via coincident detection of the  $\eta$ -meson and the recoil nucleon [18,36]. However, in the threshold region the data are significantly underestimated by this model. For both nuclei the measured cross-sections rise much faster than the predictions at energies above the breakup threshold. The size of the effects is more visible in fig. 3, where the data are divided by the impulse approximation calculation.

The large enhancement over the impulse approximation at threshold is evidence for substantial FSI effects, which are not included in the model. In the deuteron case model calculations from different groups, which include nucleon-nucleon and nucleon- $\eta$  FSI effects, have recently become available and are compared to the data in figs. 2,3. Sibirtsev *et al.* [45] have studied in detail the influence

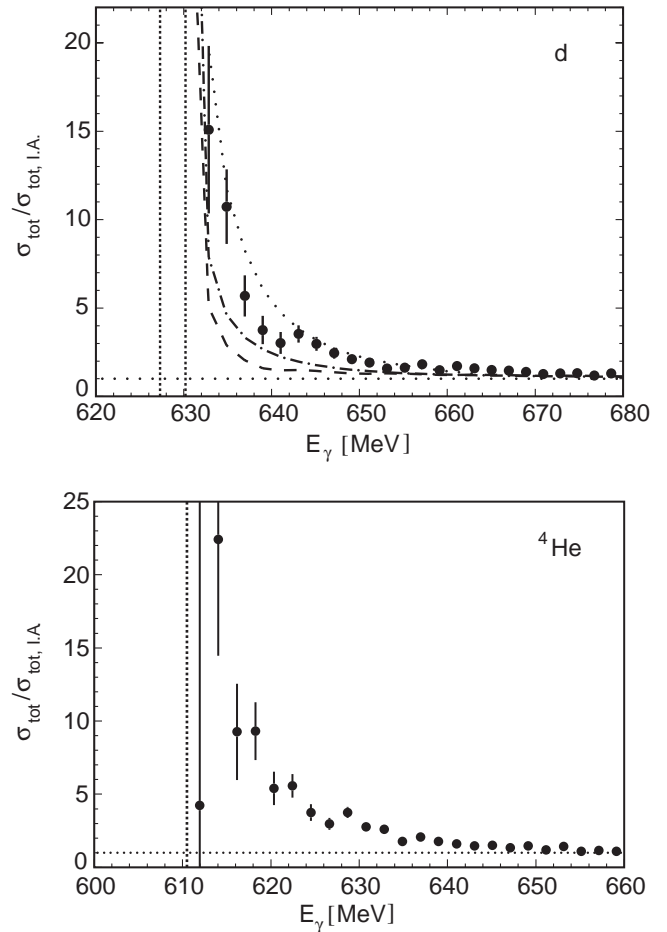


**Fig. 3.** Experimental data and model calculations normalized to the impulse approximation. The curves correspond to the same models as in fig. 2 and are also normalized to the impulse approximation.

of  $NN$  FSI on the cross-section. In agreement with our results they reproduce the cross-section in impulse approximation at higher incident photon energies but find a significant contribution of  $NN$  FSI in the threshold region. Interestingly, in contrast to hadron-induced  $\eta$  production, the  $NN$  FSI effects turn out to be rather insensitive to details of the  $NN$  potential. However, already a comparison [45] to our older low statistics data [16] suggests that the effects of  $NN$  FSI are not large enough to explain the threshold enhancement. This result is corroborated by the new data (see figs. 2,3, dash-dotted curves). This is an indication that  $N\eta$  FSI must be important. Fix and Arenhövel have calculated FSI effects from  $NN$  and  $N\eta$  rescattering [46]. They also find a significant contribution from  $NN$  rescattering but less important effects from  $N\eta$  rescattering. However, their final result (see figs. 2,3, dashed curves) still underestimates the threshold data. Very recently the same authors have presented a Faddeev-type three-body calculation of the  $NN\eta$  system with separable two-body interactions [47]. In this calculation they find that the  $\eta NN$  three-body aspects are important in the threshold region. The result of this model (see figs. 2,3,

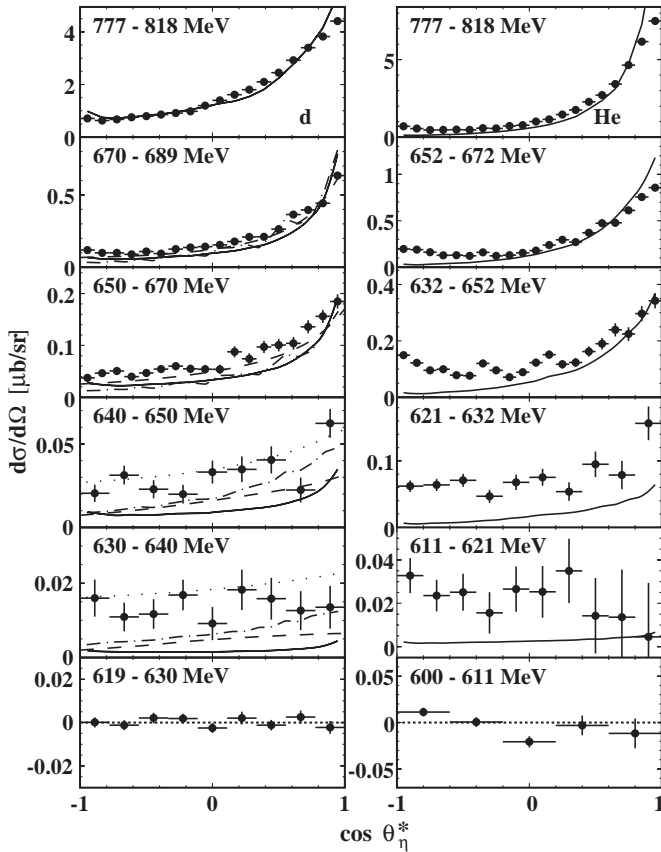


**Fig. 4.** Angular distributions of the  $\eta$  mesons in the photon-nucleus cm system. The data are divided in 5 energy bins above threshold and one bin below threshold which shows that background is negligible. Left hand side: deuterium, right hand side: helium. Solid curves: impulse approximation. The dashed, dash-dotted and dotted curves for deuterium are the model predictions from [46,45,47] as in figs. 2,3.

dotted curves) is close to the data in the threshold region but seems to underestimate it at higher incident photon energies. However, the authors mention that in order to treat explicitly the three-body aspects they have simplified some other model ingredients. In particular, they have neglected the  $d$ -wave component of the deuteron wave function and the short-range  $NN$  repulsion. Both effects are expected to reduce the pure  $s$ -wave cross-section in the threshold region. The agreement with the data therefore must be taken with some care.

Model predictions including FSI effects are not yet available for the  $^4\text{He}$  case. Here, the situation is much more complicated since calculations must account for the various exit channels  $pt$ ,  $n^3\text{He}$ ,  $dd$ ,  $pnd$ ,  $2p2n$  with the corresponding kinematical thresholds. The successive opening of the thresholds could also contribute to the observed threshold enhancement, although the shape of the relative enhancement looks quite similar for the deuteron and helium case.

Further clues to the nature of the threshold enhancement can be expected from the angular and momentum distributions of the  $\eta$ -mesons. In figs. 4,5 they are sum-

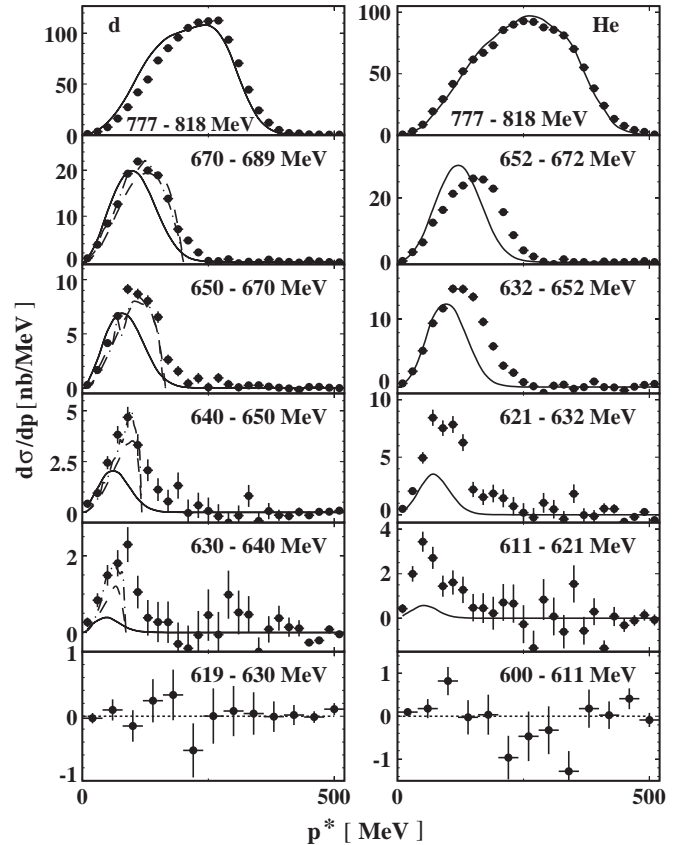


**Fig. 5.** Momentum distributions of the  $\eta$ -meson in the photon-nucleus cm frame. Solid curves: participant-spectator model folded with the experimental resolution. The dashed and dash-dotted curves for deuterium are the model predictions from [46, 45] as in figs. 2,3.

marized and compared to the results of the models. The angular distributions (see fig. 4) in the photon-nucleus cm system agree quite well with the impulse approximation at the highest incident photon energies close to the position of the  $S_{11}(1535)$  resonance. In the case of deuterium the agreement is reasonable down to photon energies around 650 MeV, but for helium an excess at backward angles develops already at higher energies. As expected, effects beyond the plane-wave approximation are larger for the strongly bound helium nucleus. Very close to threshold the measured angular distributions are almost isotropic. The shape change of the angular distributions as a function of the incident photon energy is partly due to the reaction kinematics. As already mentioned, the dominant production processes of the  $\eta$ -mesons are breakup reactions where the meson is produced on an individual nucleon that is subsequently knocked out of the nucleus. The elementary reaction on a nucleon through the  $S_{11}$  excitation is almost pure  $s$ -wave. Consequently, as long as Fermi motion is neglected the angular distributions are expected to be isotropic in the cm frame of the photon and a nucleon at rest. This behavior has been demonstrated for the deuteron [16] and is also largely true for helium, although in this case some enhancement at backward angles

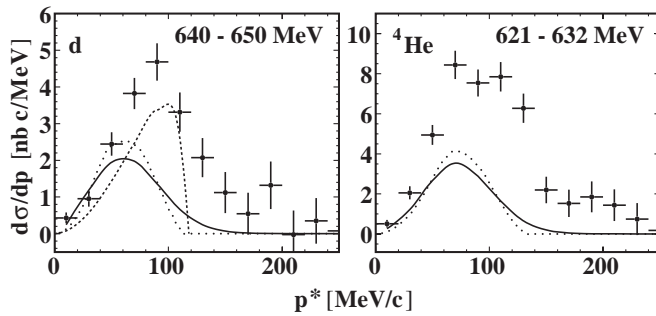


**Fig. 6.** Momentum distributions of the  $\eta$ -meson in the photon-nucleus cm frame. Solid curves: participant-spectator model folded with the experimental resolution. Dotted curves: participant-spectator approximation without finite-resolution effects. Dashed curve: calculations from ref. [46].

is visible at all incident energies [36]. The angular distribution shown here refer to the slower photon-*nucleus* rest frame so that they appear forward boosted. Since at low incident photon energies, energy conservation enforces an asymmetric selection of Fermi momenta antiparallel to the incident photon momentum, the “true” average cm frame has a velocity somewhere in between the two extremes and moves closer to the photon-nucleus frame. But this kinematical effect, which is included in the impulse approximation, does not explain the observed change in shape close to threshold. This is again an indication for significant FSI effects. However, for the photon energy range 630–640 MeV also the model results for deuterium with  $NN$  [45] or  $NN$  and  $\eta N$  [46] FSI effects predict a rise of the cross-section from backward to forward angles by a factor of 3–4, which clearly does not agree with the observed isotropy. Only the three-body calculation [47] shows a flatter behavior.

The momentum distributions in the photon-nucleus cm frame are compared to model predictions in fig. 5. Again the shape of the distributions is nicely reproduced by the participant-spectator approximation at high incident photon energies but not in the threshold region. The models with final-state interaction from [46, 45] (predictions from ref. [47] are not available) reproduce the deuterium data much better at lower energies. Here one should note, that Monte Carlo simulations of the detector response indicate that in contrast to the angular distributions the momentum distributions are significantly affected by the finite detector resolution. The plane-wave approximation was therefore folded with the detector response. This could not be done for the model predictions so that most of the disagreement between models and data at high momenta is artificial. The size of the effect is shown in fig. 6 where for one energy range folded and unfolded participant-spectator model predictions are compared to the data. The resolution effects somewhat broaden the momentum distributions but do not shift them. The model predictions from [46] are not folded with the experimental resolution which explains the sharp cutoff at large momenta.

## 4 Conclusions

It has been shown, that in  $\eta$  photoproduction from  $^2\text{H}$  and  $^4\text{He}$  the total cross-section at threshold is strongly enhanced with respect to an impulse approximation calculation. In the case of deuterium, where calculations are available, models which include  $NN$  and  $\eta N$  FSI effects account for only part of this enhancement. Only a recent three-body calculation of the  $NN\eta$  system is in better agreement with the threshold data but fails at higher incident photon energies. Both the angular and the momentum distributions of the mesons show evidence for significant final-state interaction. The enhancement bears some similarities to the threshold behavior of  $\eta$  production found in hadron-induced reactions which has been taken as tentative evidence for the formation of  $\eta$ -nucleus quasibound states. However, no firm conclusion as to FSI being strong enough to give rise to quasibound states can be drawn at this stage.

We wish to acknowledge the outstanding support of the accelerator group of MAMI, as well as many other scientists and technicians of the Institut für Kernphysik at the University of Mainz. Illuminating discussions on the theoretical interpretation of the experimental results with H. Arenhövel, A. Fix, A. Sibirtsev and C. Wilkin are gratefully acknowledged. This work was supported by the Deutsche Forschungsgemeinschaft (SFB 201), the Bundesministerium für Bildung und Forschung (BMBF, Contract No. 06 GI 475(3) I) the UK Engineering and Physical Science Research Council and the Swiss National Science Foundation.

## References

1. B. Krusche *et al.*, Phys. Rev. Lett. **74**, 3736 (1995).
2. T. Ueda, Phys. Rev. Lett. **66**, 297 (1991).
3. R.S. Bhalerao, L.C. Liu, Phys. Rev. Lett. **54**, 865 (1985).
4. L.C. Liu, Q. Haider, Phys. Rev. C **34**, 1845 (1986).
5. R.E. Chrien *et al.*, Phys. Lett. B **60**, 2595 (1988).
6. J.D. Johnson *et al.*, Phys. Rev. C **47**, 2571 (1993).
7. G.A. Sokol *et al.*, nucl-ex/9812007; nucl-ex/0011005; Izv. Akad. Nauk SSSR, Ser. Fiz. **64**, 490 (2000).
8. B. Mayer *et al.*, Phys. Rev. C **53**, 2068 (1996).
9. F. Plouin *et al.*, Phys. Rev. Lett. **65**, 690 (1990).
10. H. Calén *et al.*, Phys. Lett. B **366**, 39 (1996).
11. H. Calén *et al.*, Phys. Rev. Lett. **80**, 2069 (1998).
12. N. Willis *et al.*, Phys. Lett. B **406**, 14 (1997).
13. F. Hibou *et al.*, Eur. Phys. J. A **7**, 537 (2000).
14. M. Belligeri *et al.*, Phys. Lett. B **472**, 267 (2000).
15. J. Smyrski *et al.*, Phys. Lett. B **474**, 182 (2000).
16. B. Krusche *et al.*, Phys. Lett. B **358**, 40 (1995).
17. M. Röbig-Landau *et al.*, Phys. Lett. B **373**, 45 (1996).
18. P. Hoffmann-Rothe *et al.*, Phys. Rev. Lett. **78**, 4697 (1997).
19. J. Ajaka *et al.*, Phys. Rev. Lett. **81**, 1797 (1998).
20. T. Yorita *et al.*, Phys. Lett. B **476**, 226 (2000).
21. R. Thompson *et al.*, Phys. Rev. Lett. **86**, 1702 (2001).
22. J. Weiß *et al.*, Eur. Phys. J. A **11**, 371 (2001).
23. F. Renard *et al.*, Phys. Lett. B **528**, 215 (2002).
24. A.M. Green, S. Wycech, Phys. Rev. C **60**, 35208 (1999).

25. C. Wilkin, Phys. Rev. C **47**, R938 (1993).
26. Ch. Sauermann *et al.*, Phys. Lett. B **241**, 261 (1995).
27. M. Arima *et al.*, Nucl. Phys. A **543**, 613 (1992).
28. M. Batinić, Švarc, Few-Body Syst. **20**, 69 (1996).
29. V.V. Abaev, B.M.K. Nefkens, Phys. Rev. C **53**, 385 (1996).
30. S.A. Rakityanski *et al.*, Phys. Lett. B **359**, 33 (1995); Phys. Rev. C **53**, R2043 (1996).
31. A.M. Green *et al.*, Phys. Rev. C **54**, 1970 (1996).
32. N.N. Scoccola, D.O. Riska, Phys. Lett. B **444**, 21 (1998).
33. N.V. Shevchenko *et al.*, Eur. Phys. J. A **9**, 143 (2000).
34. V. Yu. Grishina *et al.*, Phys. Lett. B **475**, 9 (2000).
35. H. Garcilazo, M.T. Pena, Phys. Rev. C **63**, R21001 (2001).
36. V. Hejny *et al.*, Eur. Phys. J. A **6**, 83 (1999).
37. I. Anthony *et al.*, Nucl. Instrum. Methods A **301**, 230 (1991).
38. Th. Walcher, Prog. Part. Nucl. Phys. **24**, 189 (1990).
39. R. Novotny, IEEE Trans. Nucl. Sci. **38**, 379 (1991).
40. A.R. Gabler *et al.*, Nucl. Instrum. Methods A **346**, 168 (1994).
41. R. Brun *et al.*, GEANT, Cern/DD/ee/84-1, 1986.
42. B. Krusche *et al.*, Z. Phys. A **351**, 237 (1995).
43. M. Lacombe *et al.*, Phys. Lett. B **101**, 139 (1981).
44. J.S. McCarthy *et al.*, Phys. Rev. C **15**, 1396 (1977).
45. A. Sibirtsev *et al.*, Phys. Rev. C **64**, 24006 (2001).
46. A. Fix, H. Arenhövel, Z. Phys. A **359**, 427 (1997).
47. A. Fix, H. Arenhövel, Nucl. Phys. A **697**, 277 (2002).